**Quarterly Progress Report**

This report covers the period of June 15, 2015 to September 14, 2015

Submitted to

**The Office of Naval Research**

**Project Title : Noise of High-Performance Aircraft at Afterburner**

**Principal Investigator**

Dr. Christopher Tam

Department of Mathematics

Florida State University

Email: tam@math.fsu.edu

**Grant Monitor**

Dr. John Spyropoulous

Email: John.Spyropoulous@jsf.mil

**Technical Representative**

Dr. Joseph Doychak

Email: joseph.doychak@navy.mil

1

This progress report consists of two parts. They are:

1. Development of a stochastic broadband entropy wave generation model boundary condition. The purpose of this model boundary condition is to provide support for an investigation of indirect combustion noise generation in a military styled supersonic nozzle by numerical simulation.

2. Analyze NAVAIR F-18E noise data. Special attention is focused on the difference between the engine noise of this aircraft and the noise of a standard hot supersonic laboratory jet.

**Part 1. Development of a stochastic model entropy wave boundary condition**

The task of the first year research of this project is to develop a stochastic broadband entropy wave generation model boundary condition. This model boundary condition is needed in the second year research on the generation of indirect combustion noise in a military-styled nozzle. Figure 1 shows randomly distributed hot and cold blobs convected into a nozzle by the mean flow. The mean flow is highly non-uniform in the nozzle. It is known that the passage of hot and cold entropy wave blobs through a non-uniform mean flow would lead to the generation of indirect combustion noise. Details of the generation process, its effectiveness and its dependence on the geometry and flow parameters of the nozzle are the subject of the second year research. In a numerical simulation, the boundary condition on the left boundary of the nozzle in figure 1 is responsible for generating the incoming random entropy wave field. We would like to report that such a model boundary condition has now been developed.
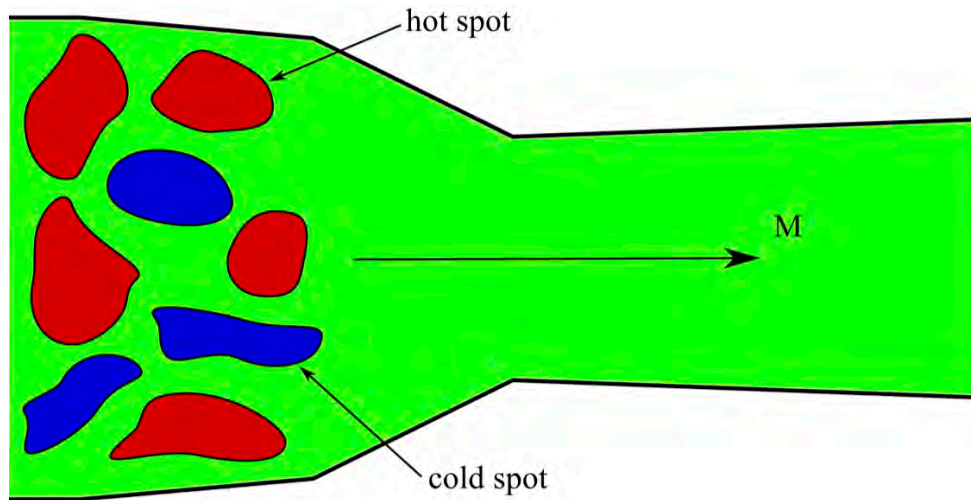


Figure 1. A field of random entropy wave blobs entering the left boundary of a military-styled nozzle.

A stochastic field is characterized only by it statistical properties. In using our model boundary condition, one is allowed to prescribe the following single-point and two-point statistics.

*Single-point statistics*

Figure 2 shows a mean flow in the x-direction. The y-z plane is perpendicular to the flow. Once created, the random entropy wave field is convected downstream past the y-z plane of figure 2. The temperature fluctuations at any instant of time is random in the y-z plane. However, the time average of the square of temperature fluctuations, $\overline{T'^2}$ , (an overbar denotes time average) at any point is the same. It is a quantity that can be prescribed by the user of the model boundary condition. In addition, our model allows the user to specify the spectrum, $S(f)$ , of temperature fluctuations at any point on the y-z plane. Thus, the model boundary condition we have developed allows one to specify single-point statistics $\overline{T'^2}$ and $S(f)$.



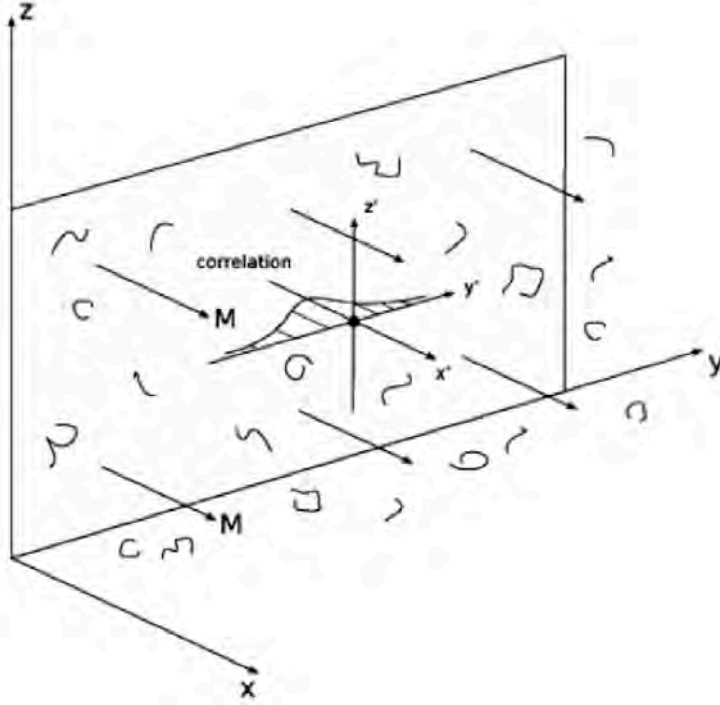Figure 2. The *y-z* plane is perpendicular to the mean flow in the *x*-direction. The flow Mach number is *M*. The spatial cross-correlation function in the *y*-direction at a point in the *y-z* plane is shown in the form of a bell shaped curve.

*Two-point statistics*

To characterize the size of the entropy blobs to be created, our model permits the user to prescribe a two-point spatial correlation function of the fluctuating temperature in each of the y and z directions at any point on the *y-z* plane. This is shown in figure 2. The bell shaped curve is the two-point spatial correlation function in the y-direction. The half-width of this function is, statistically, the average size of the entropy blobs.

Our stochastic model broadband entropy wave generation boundary condition has been successfully tested. The tests consist of prescribing a value of $\overline{T'^2}$ and a frequency spectrum $S(f)$. In addition, a two-point spatial correlation function in the form of a Gaussian function in the y and z directions is also specified. The model is then used to generate a random field of temperature fluctuations in space and time. The time histories of temperature fluctuations at a number of selected points and along a line in the y-direction are measured. These measured data are then processed to compute $\overline{T'^2}$ and $S(f)$ as well as $\overline{T'(x,y',t)T'(x,y'',t)} = F(x,y'-y'')$, the spatial correlation function in the y-direction. All these statistics are found to agree well with the corresponding input values and functions. Figure 3 shows the temperature distribution in the y-z plane at a particular instant of time in one of our tests. In this test, the mean flow at Mach number 0.3 enters the computational domain at $45^0$ to the x-axis or parallel to the diagonal of the computational domain.
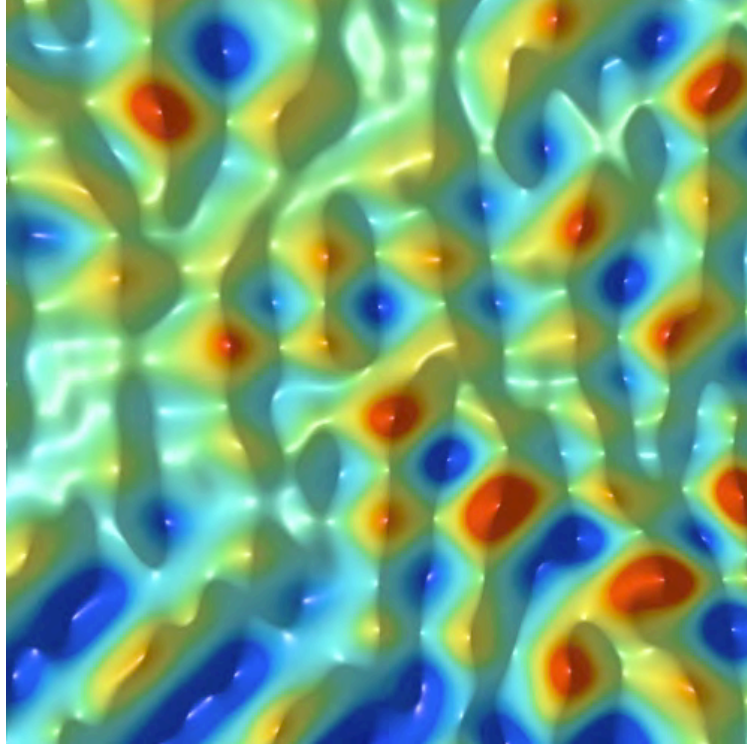


Figure 3. A random field of entropy blobs generated by the model entropy wave generation boundary condition developed in the present research effort.

We are in the process of carrying out a series of second level tests. In these tests, our model boundary condition is applied only to the boundary regions of two-dimensional simulations. A uniform inflow at a prescribed Mach number flows over the entire computational domain. Initially, there is no entropy blob in the computational domain. The entropy blobs are generated by the model boundary condition beginning at time zero (see figure 4). The flow field and its convected entropy blobs are marched in

time using the DRP scheme. The computation continues until the entire computational domain is filled by entropy blobs. Our plan is to measure $T'(t)$ at selected points in the computational domain. These time history data will be used to compute the intensity $\overline{T'^2}$, the spectrum $S(f)$ and the two point spatial correlation function $F(x, y' - y'')$. Once these tests are completed, we will start our numerical simulation of indirect combustion noise generation in a military-styled nozzle.
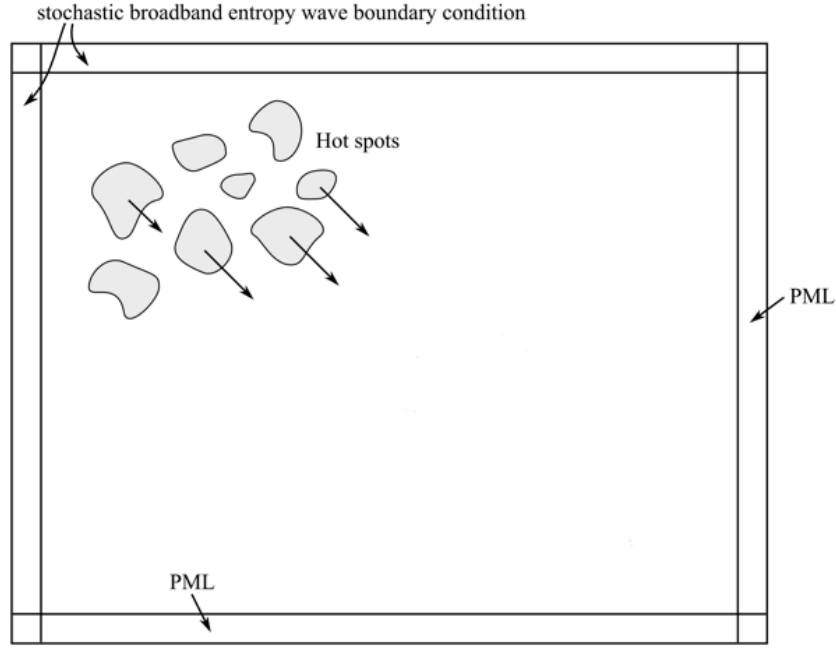


Figure 4. Entropy blobs generated by our stochastic model boundary condition. These entropy blobs, once created at the boundary region, are convected downstream by the mean flow.

## Part 2. Analysis of the F-18E aircraft noise

In our last quarterly progress report, we concluded that at power setting of 80N2 and higher, jet noise is the dominant source of F-18E aircraft noise. In addition, at power setting of 80N2 the dominant jet noise components are essentially the same as those of standard high temperature supersonic laboratory jets. These jets have two dominant sources of noise. They are the fine scale turbulence noise and the noise from the large turbulence structures of the jet flow. Figure 5 illustrates the principal directions of radiation of the two dominant noise components. The fine scale turbulence noise radiates to the sideline and in the forward directions. The large turbulence structures noise is primarily in the form of Mach wave radiation. It is confined to a Mach cone in the downstream direction. Figures 6 and 7 show comparisons of the noise spectrum of the F-18E jet noise measured at inlet angle of $77^0$ and $141^0$ and the similarity spectra. There are reasonably good agreements. They support the contention that the dominant noise components are basically the same as those of laboratory jets.
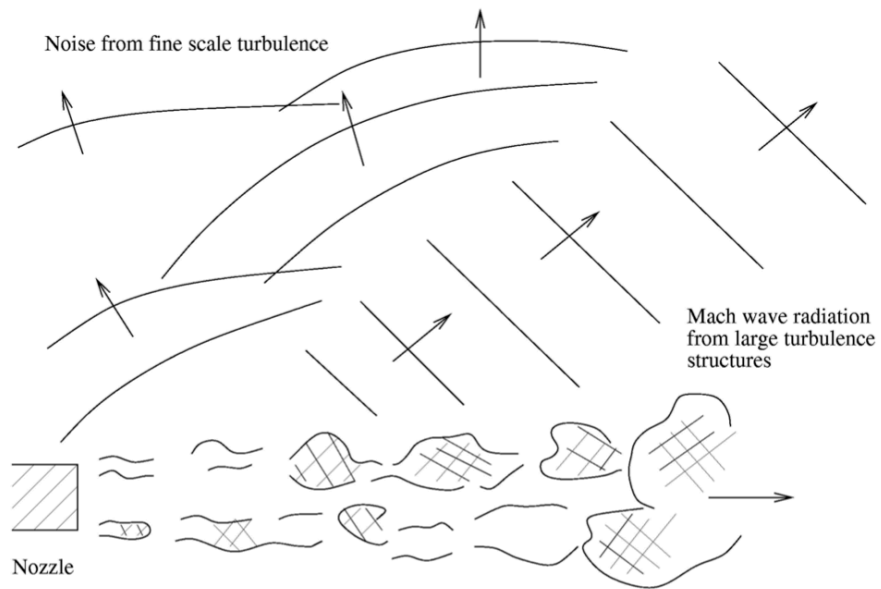
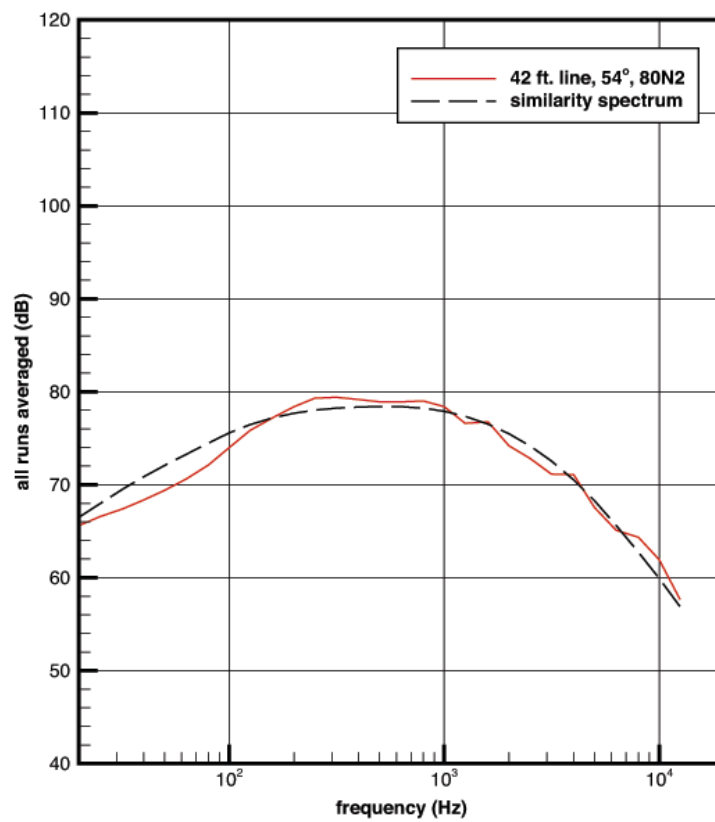Figure 5. The two-noise source model of high-speed jets



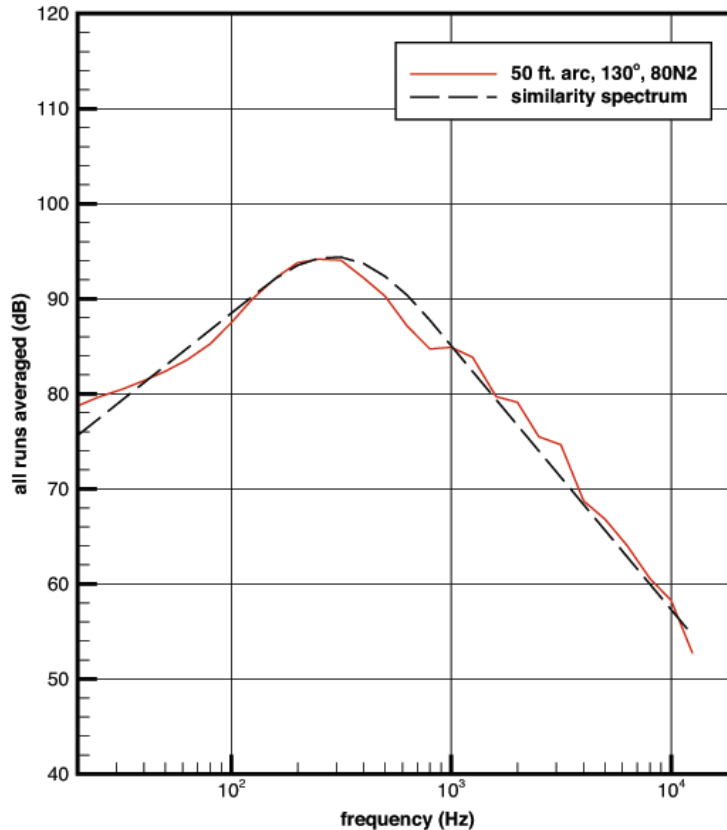Figure 6. Noise spectrum at 80N2 power setting in the direction of 65 degrees.

Figure 7.  Noise spectrum at 80N2 power setting in the direction of $130^0$

Another conclusion of the preliminary report contained in the last quarterly report is that the noise of F-18E aircraft at Mil and MaxAB engine setting is very different from that of a laboratory jet. We have now performed a somewhat detailed analysis of the noise spectra at these two higher power settings. Below is a report on some of the characteristic features of the noise spectra at Mil and MaxAB power level.

A. *Some characteristic features of the noise spectra in the forward and sideline directions.*

Upon examining all the available spectra, it is our conclusion that the dominant noise components of the jet at Mil and MaxAB power level are the same except that the intensities are higher at MacAB. In the forward and sideline directions, there is fine scale turbulence noise. But it is not the dominant component. Figures 8, 9, 10 and 11 show the noise spectra at inlet angle $31^0$, $40^0$, $54^0$ and $77^0$ at MaxAB engine setting. Included in these plots is the fine scale turbulence noise similarity spectrum. Figures 12, 13, 14, and 15 show similar spectra at Mil power level. Clearly, the most dominant feature of these spectra is a high intensity relatively narrow peak.  The peak protrudes high above the fine scale turbulence noise. The peak frequency varies with the direction of radiation. The narrowness of the spectral peak and the increase in peak frequency with increase in the angle of radiation (inlet angle) suggests that this noise component could be broadband shock cell noise (they have the same characteristics). Shock cell noise is generated by the

7

interaction of the large turbulence structures of the jet flow and the quasi-periodic shock cells as the former propagate downstream through the latter. In the F-18E jet, we are, however, not sure if the peak is really created by turbulence-shock cells interaction. It could be due to the interaction of entropy blobs and shock cells. A more in-depth study is required to determine the underlying noise generation mechanism.
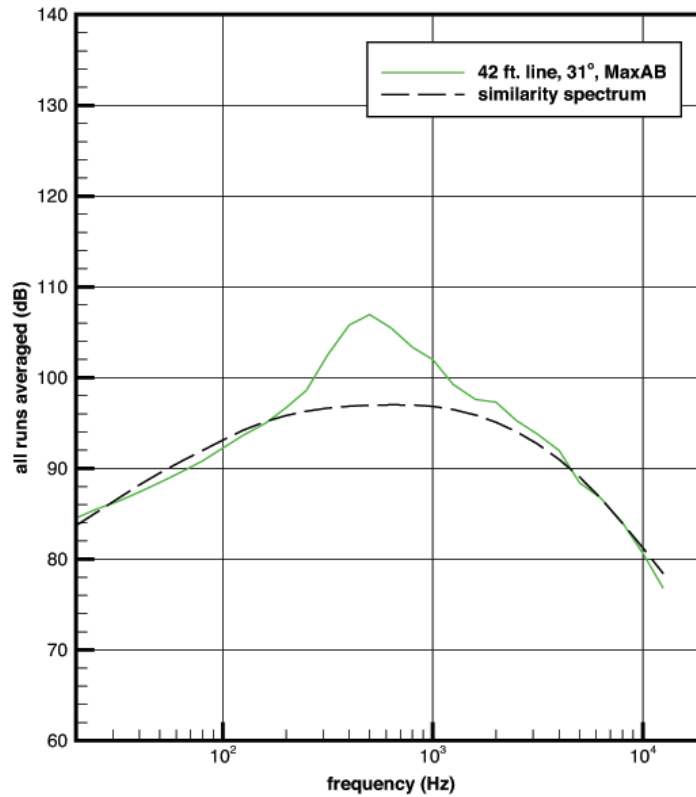


Figure 8. Noise spectrum at $31^0$ at MaxAB power setting. Dotted line is the similarity spectrum of fine scale turbulence noise.
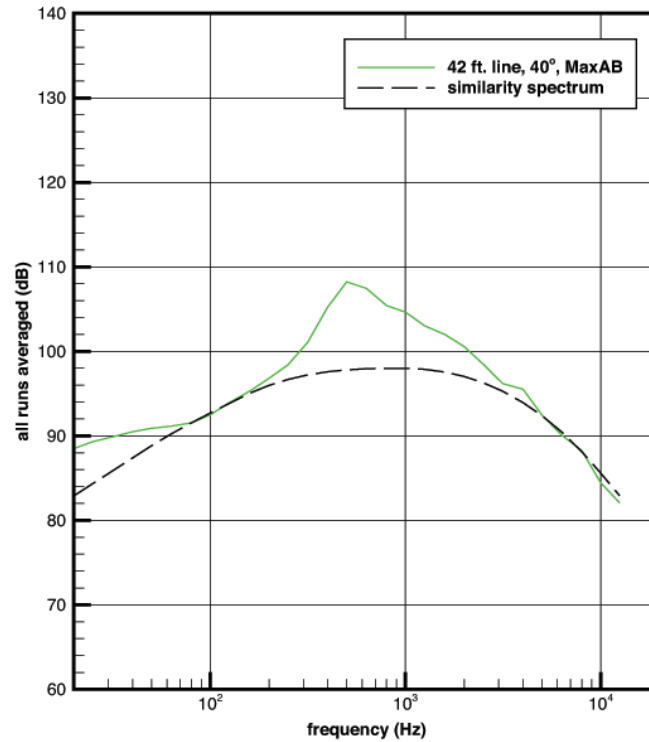
Figure 9. Noise spectrum at $40^0$ at MaxAB power setting. Dotted line is the similarity spectrum of fine scale turbulence noise.
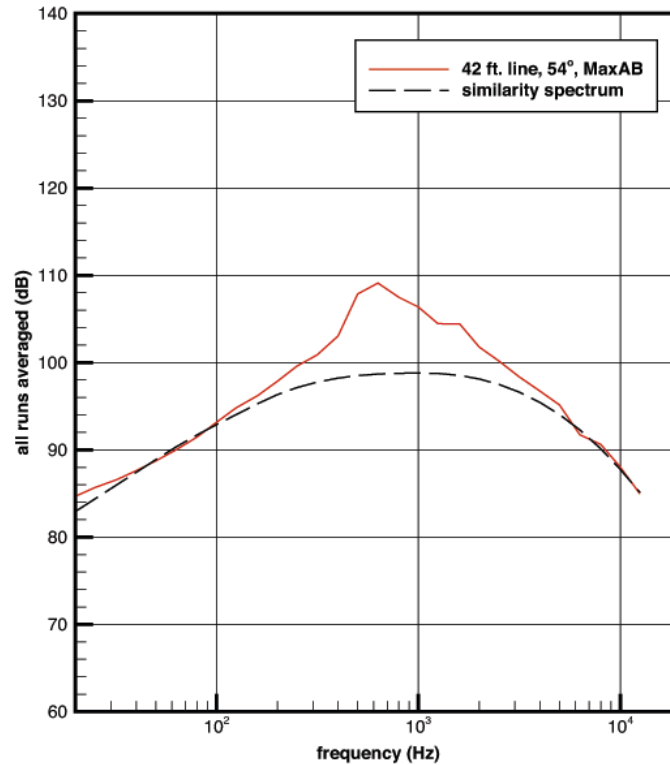


Figure 10. Noise spectrum at $54^0$ at MaxAB power setting. Dotted line is the similarity spectrum of fine scale turbulence noise.
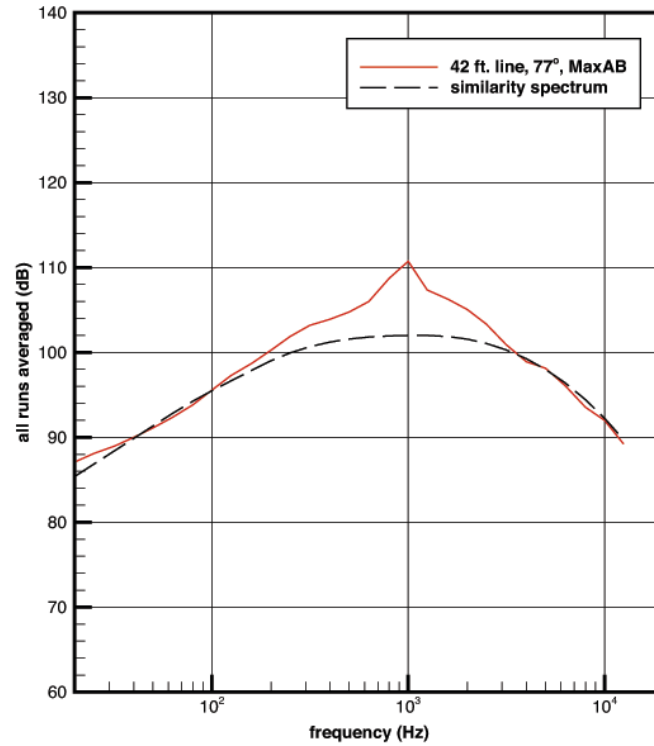
Figure 11. Noise spectrum at $77^0$ at MaxAB power setting. Dotted line is the similarity spectrum of fine scale turbulence noise.
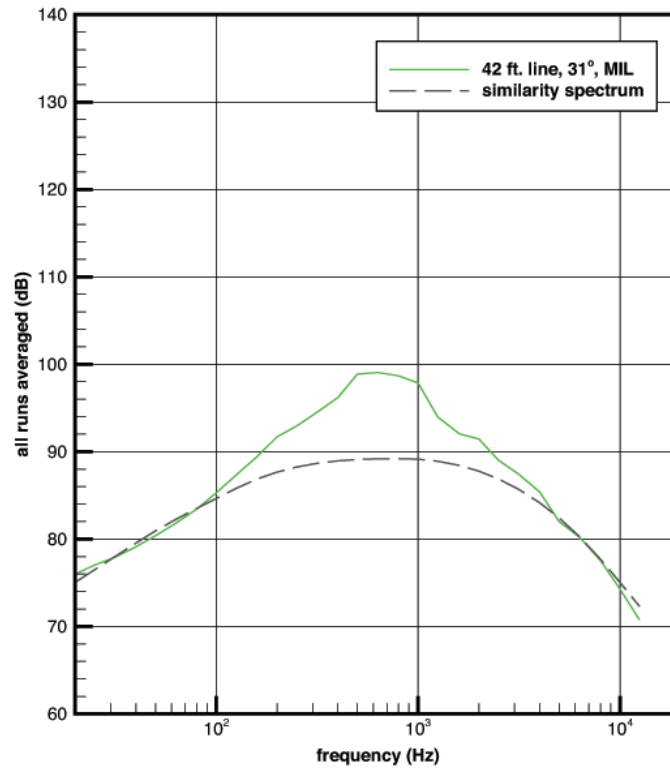


Figure 12. Noise spectrum at $31^0$ at Mil power setting. Dotted line is the similarity spectrum of fine scale turbulence noise.
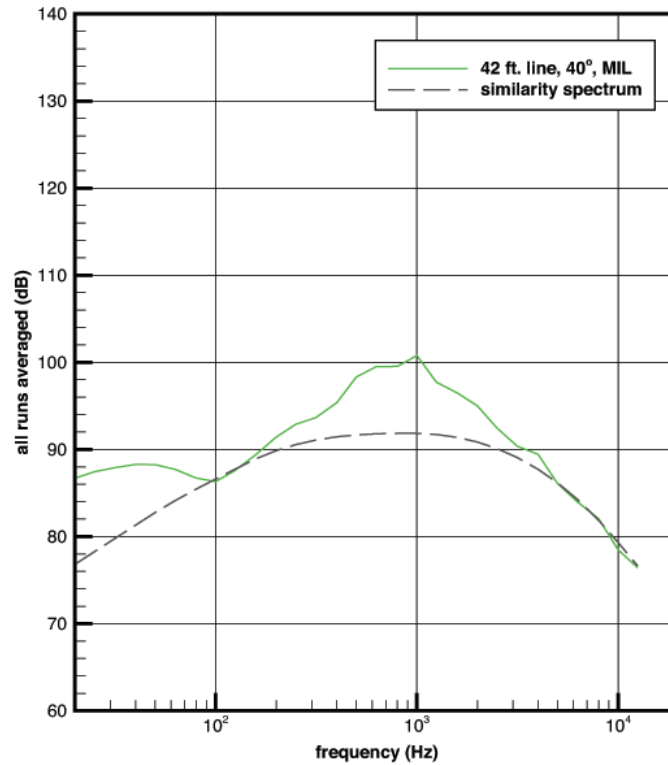
Figure 13. Noise spectrum at $40^0$ at Mil power setting. Dotted line is the similarity spectrum of fine scale turbulence noise.
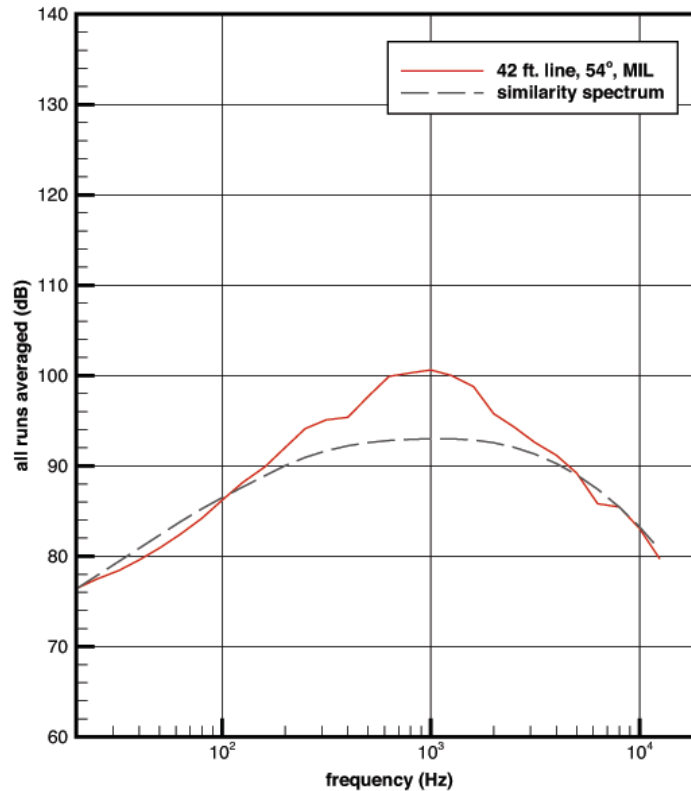


Figure 14. Noise spectrum at $54^0$ at Mil power setting. Dotted line is the similarity spectrum of fine scale turbulence noise.
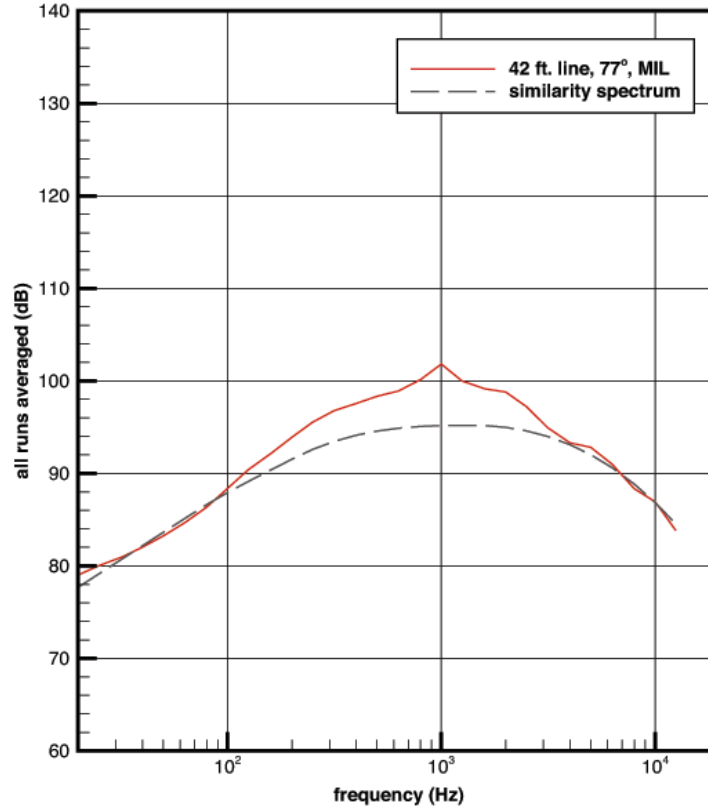
Figure 15. Noise spectrum at $77^0$ at Mil power setting. Dotted line is the similarity spectrum of fine scale turbulence noise.

*B. Some characteristic features of the noise spectra in the aft directions.*

A careful review of all the noise spectra in the directions of $90^0$ to $160^0$ reveals that the noise sources and radiation characteristics are quite different from those of standard laboratory jets. A list of the most prominent features are summarized below.

(i) Evidence of two dominant noise components in the aft directions

Figure 16 shows the noise spectra at MaxAB for the directions of radiation from $125^0$ inlet angle to $160^0$ angle. It should be clear that the spectra exhibit two independent peaks. The spectra of $\theta = 125^0$, $130^0$, $135^0$ and $141^0$ have a peak around 3 kHz. The spectra of $\theta = 145^0$, $150^0$, $155^0$ and $160^0$ have a peak at around 1.2 kHz. Figure 17 shows the corresponding spectra for $\theta = 125^0$ to $160^0$ for the noise of the aircraft operating at Mil power. Again there appears to be two peaks at similar peak frequencies as those at MaxAB power.

12
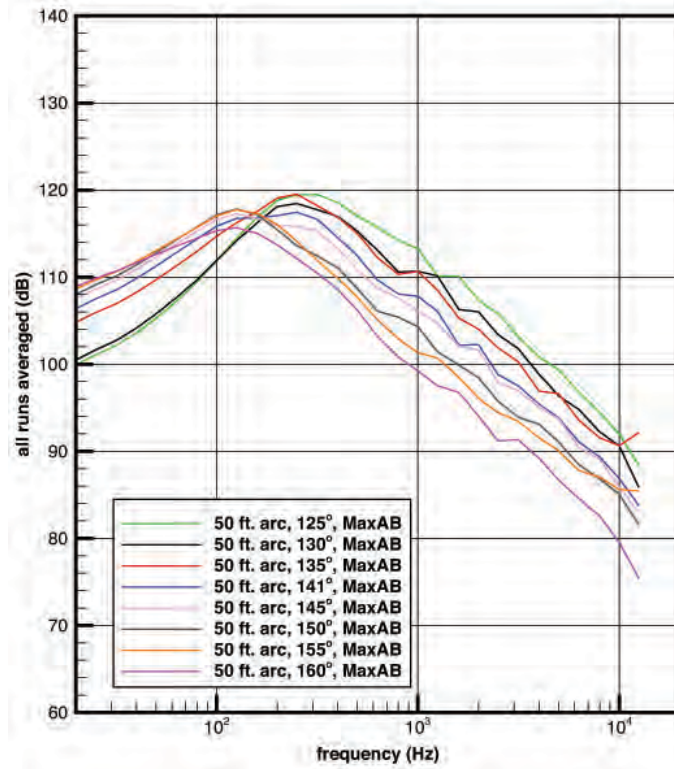
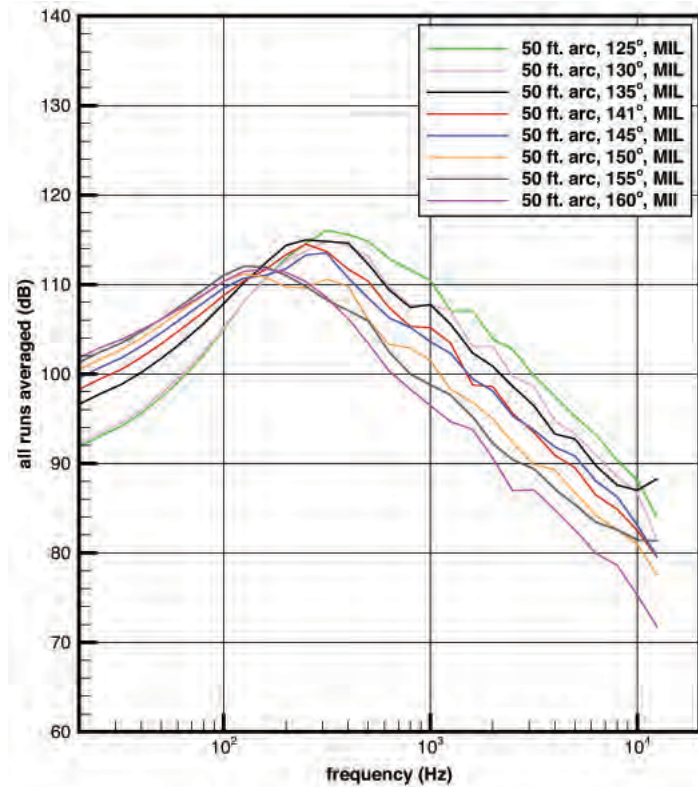Figure 16. Noise spectra at MaxAB power at inlet angle $125^0$ to $160^0$ showing two independent peaks.



Figure 17. Noise spectra at Mil power at inlet angle $125^0$ to $160^0$ showing two independent peaks.

Figure 18 shows the spectra at $\theta = 135^0$, $141^0$, $145^0$ and $150^0$ at MaxAB power. The spectra at $\theta = 135^0$ and $150^0$ clearly have a single dominant peak. On the other hand, the spectra at $\theta = 141^0$ and $145^0$ have two peaks providing irrefutable evidence that there are two dominant sources that radiate noise in the aft directions. Shown in figure 19 are spectra at the four angles $\theta = 141^0$, $145^0$, $150^0$ and $155^0$ at Mil power. The spectra at $\theta = 141^0$ and $155^0$ have double peaks. Again this suggesting strongly the at Mil power, there are two dominant noise sources.
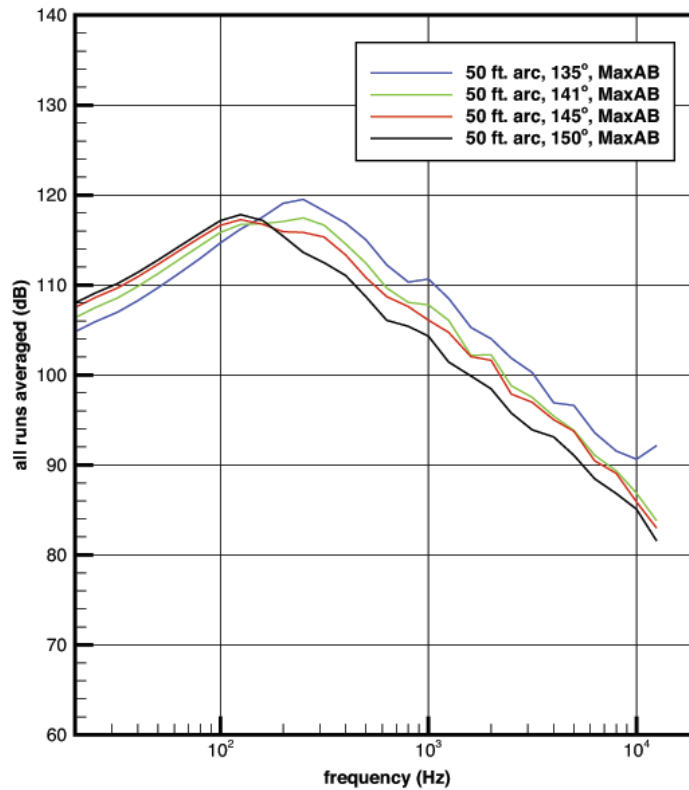


Figure 18. Noise spectra at four angular directions, $\theta = 135^0$, $141^0$, $145^0$ and $150^0$ at MaxAB power level showing the transition from one dominant peak to the other dominant peak.
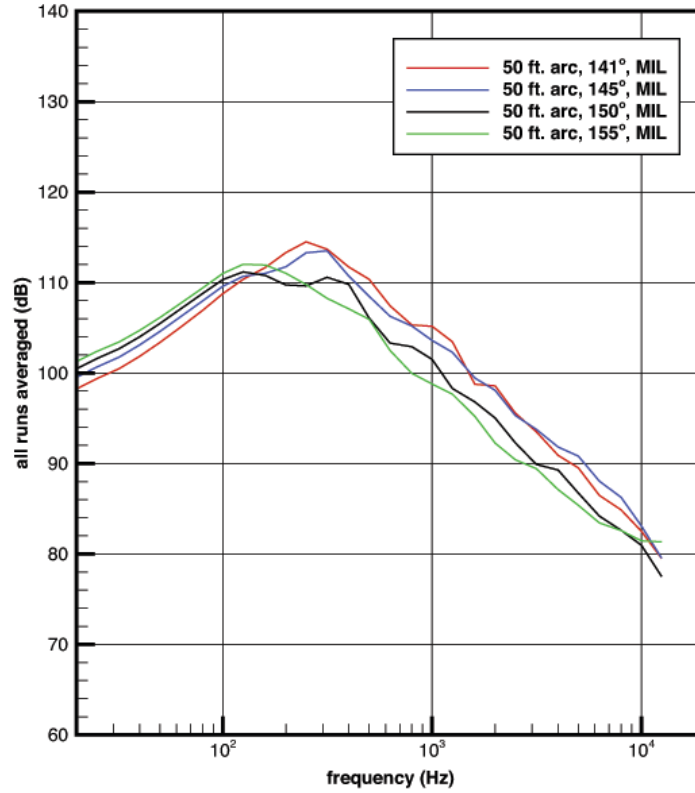
Figure 19. Noise spectra at four angular directions, $\theta = 141^0$, $145^0$, $150^0$ and $155^0$ at Mil power level showing the transition from one dominant peak to the other dominant peak.

 (2) Noise from the large turbulence structures of the jet flow

For standard hot supersonic laboratory jets, the dominant noise component is from the large turbulence structures of the net flow. This is also true when the engine of the F-18E aircraft operating at 82N2 power as reported before. We, therefore, expect one of the two dominant noise component at MaxAB and Mil power is from the large turbulence structures of the jet flow. Figures 20, 21, 22 and 23 are noise spectra at MaxAB power for $\theta = 130^0$, $141^0$, $145^0$ and $150^0$. Fitted to these spectra is the similarity spectrum of the large turbulence structures noise of standard laboratory jets. The spectrum peak is at approximately 300 Hz. Generally speaking, there is good fit in all the above case. We also would like to report that there is similar good fit for $\theta = 125^0$ and $\theta = 160^0$ as well. At Mil power, the similarity spectrum of large turbulence structures noise is also a good fit to the noise spectra at $\theta = 125^0$ to $\theta = 160^0$ with the peak frequency at again around 300 Hz. The good fit in all the cases we have data indicates that the noise from the large turbulence structures of the jet flow remains a dominant noise component of the F-18E aircraft.
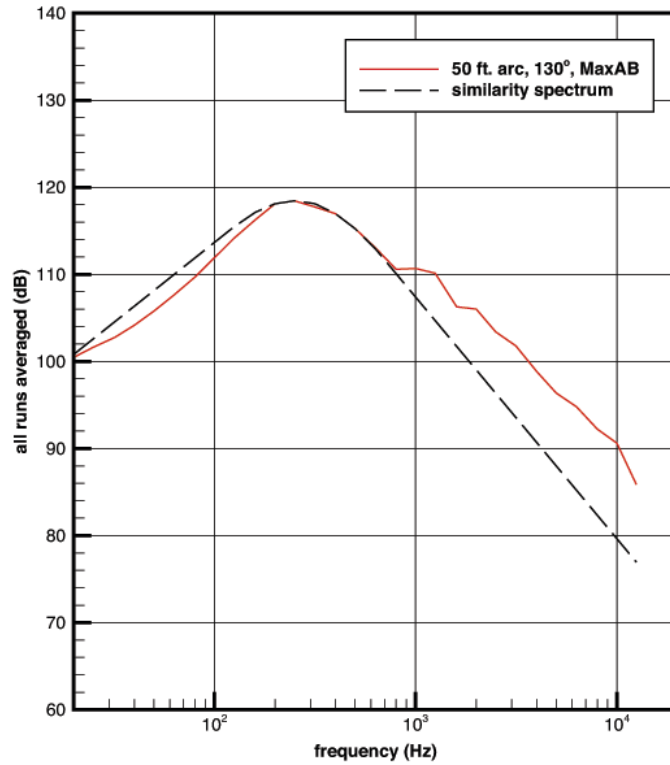
Figure 20. Comparison between measured spectrum at $130^0$ at MaxAB power and the similarity spectrum of the large turbulence structures noise of the jet flow.
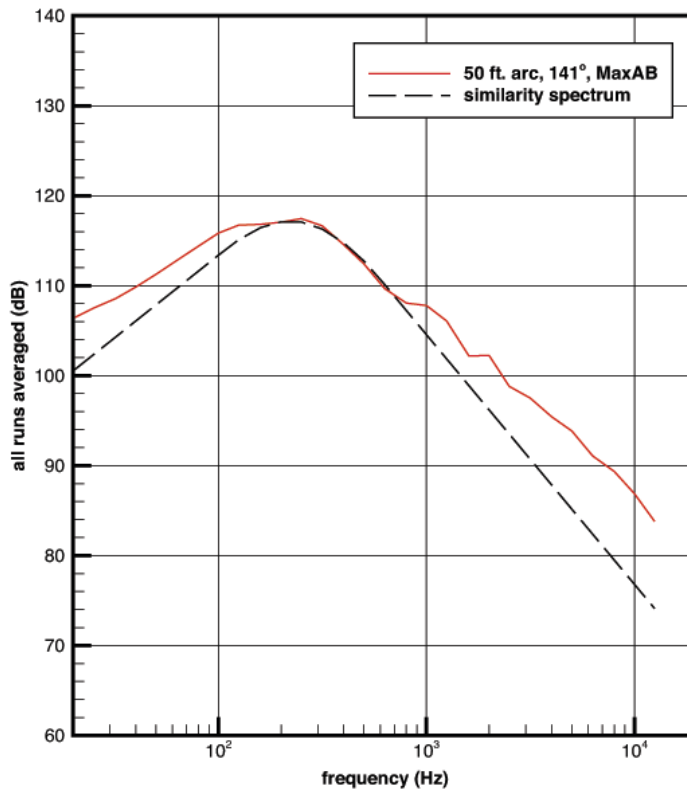


Figure 21. Comparison between measured spectrum at $141^0$ at MaxAB power and the similarity spectrum of the large turbulence structures noise of the jet flow.
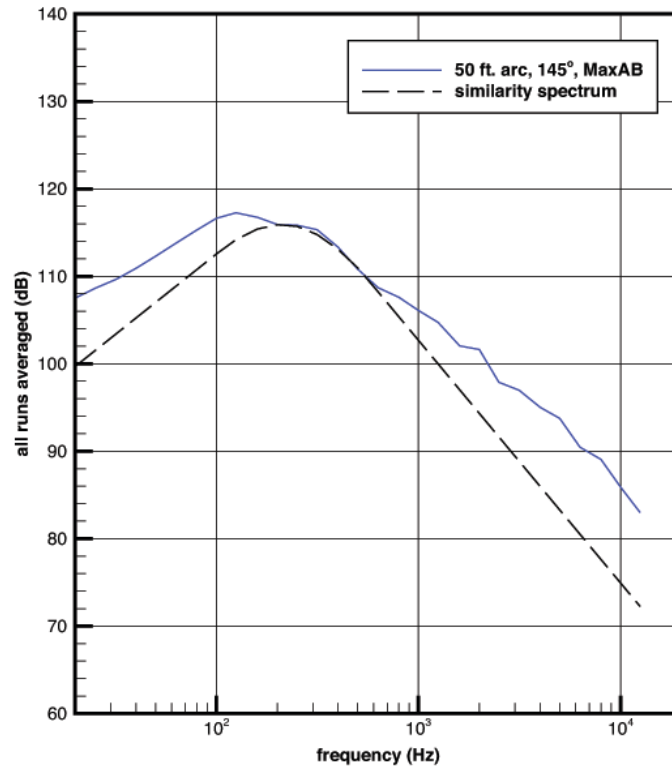
16

Figure 22. Comparison between measured spectrum at $145^0$ at MaxAB power and the similarity spectrum of the large turbulence structures noise of the jet flow.
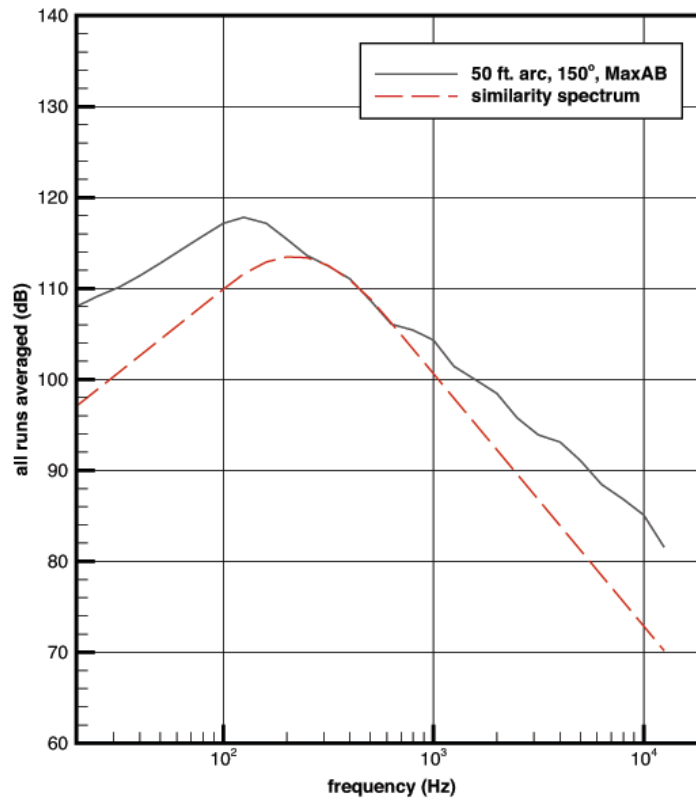


Figure 23. Comparison between measured spectrum at $150^0$ at MaxAB power and the similarity spectrum of the large turbulence structures noise of the jet flow.

17

Figure 24. Comparison between measured spectrum at $135^0$ at Mil power and the similarity spectrum of the large turbulence structures noise of the jet flow.



Figure 25. Comparison between measured spectrum at $141^0$ at Mil power and the similarity spectrum of the large turbulence structures noise of the jet flow.

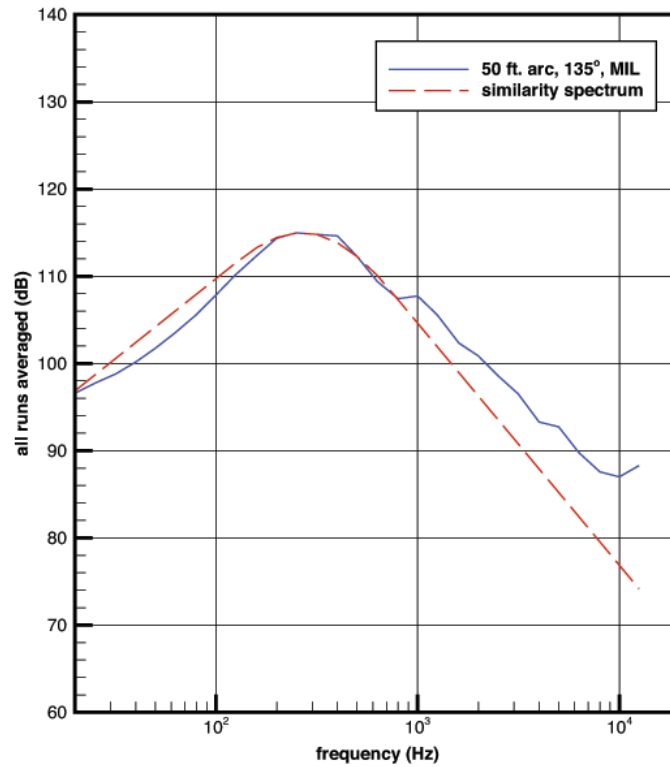Figure 26. Comparison between measured spectrum at $150^0$ at Mil power and the similarity spectrum of the large turbulence structures noise of the jet flow.



Figure 27. Comparison between measured spectrum at $155^0$ at Mil power and the similarity spectrum of the large turbulence structures noise of the jet flow.
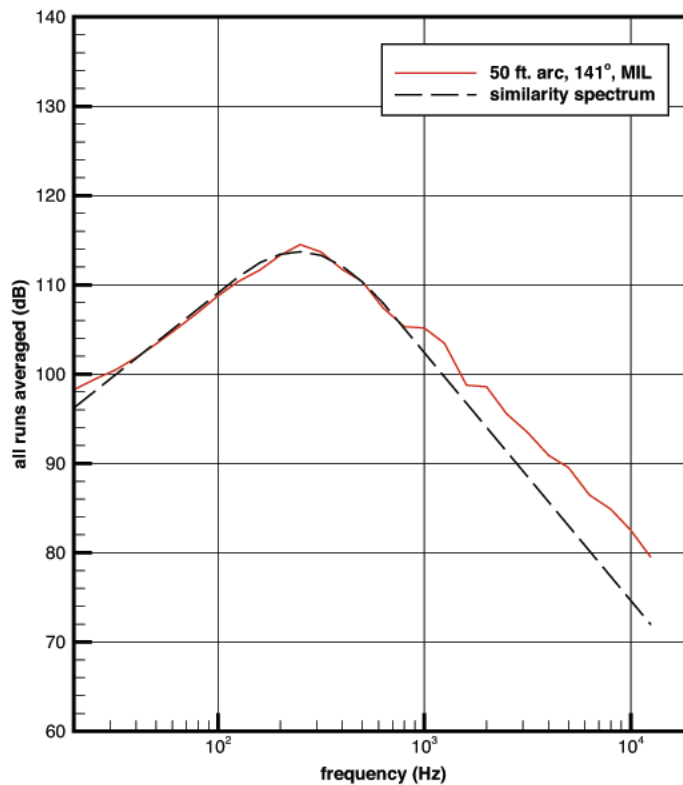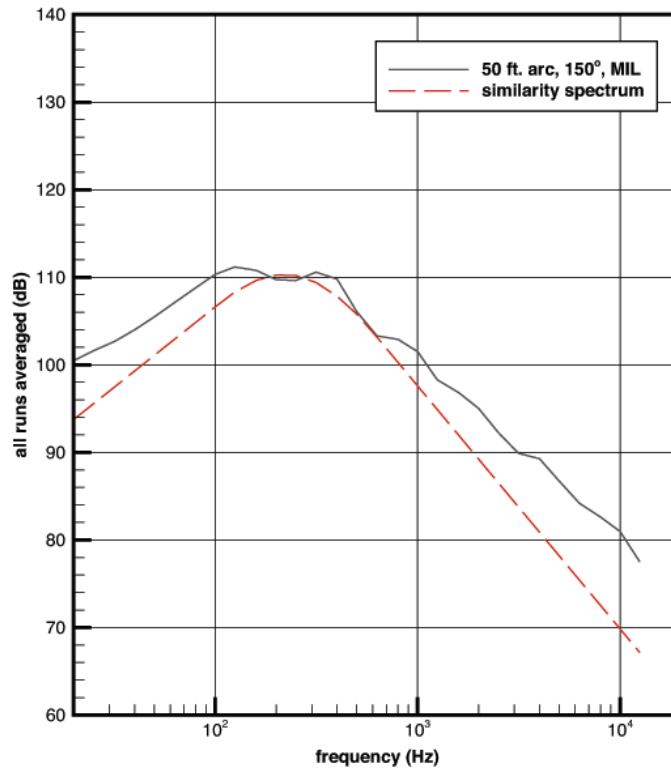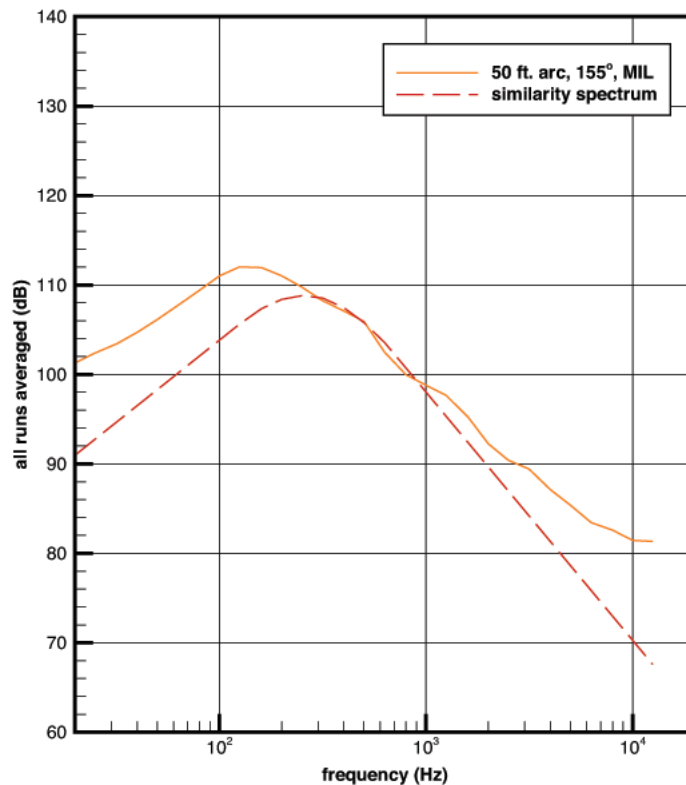
(iii) A high frequency noise component

In addition to the large turbulence structures noise, the noise spectra in figures 20 to 27 show the presence of a high frequency noise component that does not exist in standard hot supersonic laboratory jets. This noise component has frequency higher than that of the large turbulences structures noise. Most of the noise of this component shows up in the frequency range of higher than 1,000 Hz. The level of this high frequency noise component is highest at low inlet angle of radiation. It only appears in aft directions. The maximum noise level reduces as the angle of radiation increases. At this time, we do not know what is the source of this high frequency noise component. However, it is highly possible that it is combustion related as it becomes most prominent when the engine is operating at the highest fuel burnt rate.


**Future research**

Our research plan for the next quarter is to continue our research activities in the development of a stochastic entropy wave generation boundary condition as well as further analysis of the NAVAIR F-18E noise data.

# REPORT DOCUMENTATION PAGE

The public reporting burden for this collection of information is estimated to average 1 hour per response, including the time for reviewing instructions, searching existing data sources, gathering and maintaining the data needed, and completing and reviewing the collection of information. Send comments regarding this burden estimate or any other aspect of this collection of information, including suggestions for reducing the burden, to Department of Defense, Washington Headquarters Services, Directorate for Information Operations and Reports (0704-0188), 1215 Jefferson Davis Highway, Suite 1204, Arlington, VA 22202-4302. Respondents should be aware that notwithstanding any other provision of law, no person shall be subject to any penalty for failing to comply with a collection of information if it does not display a currently valid OMB control number.
**PLEASE DO NOT RETURN YOUR FORM TO THE ABOVE ADDRESS.**

| 1. REPORT DATE (DD-MM-YYYY) | 2. REPORT TYPE | 3. DATES COVERED (From - To) |
|---|---|---|
| 10/07/2015 | Quarterly Progress Report | 06/15/2015 to 08/14/2015 |

**4. TITLE AND SUBTITLE**

Noise of High-Performance Aircraft at Afterburner

**5a. CONTRACT NUMBER**

**5b. GRANT NUMBER**

N00014-15-1-2008

**5c. PROGRAM ELEMENT NUMBER**

**6. AUTHOR(S)**

Tam, Christopher

**5d. PROJECT NUMBER**

**5e. TASK NUMBER**

**5f. WORK UNIT NUMBER**

**7. PERFORMING ORGANIZATION NAME(S) AND ADDRESS(ES)**

Sponsored Research Administratiion
Florida State University
874Traditions Way
Tallahassee, FL 32306-4166

**8. PERFORMING ORGANIZATION REPORT NUMBER**

035259

**9. SPONSORING/MONITORING AGENCY NAME(S) AND ADDRESS(ES)**

Office of Naval Research AEROSPACE SCIENCE RESEARCH DIV
875 N. Randolph Street
Arlington, VA 22203-1995

**10. SPONSOR/MONITOR'S ACRONYM(S)**

ONR

**11. SPONSOR/MONITOR'S REPORT NUMBER(S)**

**12. DISTRIBUTION/AVAILABILITY STATEMENT**

DISTRIBUTION STATEMENT A: Approved for public release: distribution unlimited

**13. SUPPLEMENTARY NOTES**

**14. ABSTRACT**

The noise of a F18E aircraft is studied and analyzed. The main objective is to find out whether the noise has the same dominant noise components as those of a laboratory supersonic jet. The noise spectra at 3 power settings were studied. It is found that at low power, the dominant noise componets are very similar to those of a laboratory jet. But at hight power, there are significant differences.

**15. SUBJECT TERMS**

| 16. SECURITY CLASSIFICATION OF: | | | 17. LIMITATION OF ABSTRACT | 18. NUMBER OF PAGES | 19a. NAME OF RESPONSIBLE PERSON |
|---|---|---|---|---|---|
| a. REPORT | b. ABSTRACT | c. THIS PAGE | | | Christopher Tam |
| U | U | U | UU | 21 | 19b. TELEPHONE NUMBER (Include area code) 850-644-2455 |